Electronic Supplementary Material (ESI) for Journal of Materials Chemistry C.

Supporting Information

Tuning White Light Emission and Band Gap in One-Dimensional Organic Metal Halide $(C_6H_{13}N_4)_3Pb_2Br_7$ under Pressure

Nan Li,[a] Yuanyuan Fang,[a] Long Zhang,*[a] Kai Wang,[ab] and Bo Zou*[a]

[a]State Key Laboratory of Superhard Materials, College of Physics, Jilin University, Changchun 130012, China.

[b]Shandong Key Laboratory of Optical Communication Science and Technology, School of Physics Science and Information Technology, Liaocheng University, Liaocheng 252000, China.

AUTHOR INFORMATION

Corresponding Author

*To whom correspondence should be addressed.

Long Zhang, E-mail: zhanglong@jlu.edu.cn

Bo Zou, E-mail: zoubo@jlu.edu.cn

Experimental details

Sample preparation and high-pressure generation

The crystals of $(HMTA)_3Pb_2Br_7$ were synthesized according to the previous reports.[1] The *in situ* high-pressure tests were carried out by using a symmetric diamond anvil cell (DAC). The culet size of the DAC was 400 microns. To create the sample chamber, a hole with a 150-micron diameter was drilled into a T301 steel gasket that had been pre-indented with a 40-micron thickness. The pressure-transmitting medium (PTM) for our *in situ* high-pressure PL, UV-Vis absorption, Time-resolved PL, and angle-dispersive X-ray diffraction experiment was silicone oil with a viscosity of 10 cSt (25 °C). Raman experiment used argon as the PTM. Using the ruby fluorescence method, ruby balls were placed into the chamber to calculate the pressure.

In situ high-pressure optical characterizations

High-pressure PL measurements: A 355 nm excitation laser with a power of 10 mW was used to excite PL experiments.

High-pressure UV-Vis absorption measurements: A deuterium-halogen light source was used to measure UV-Vis absorption. The spectrometer in the fiber is an Ocean Optics QE65000 spectrometer.

High-pressure Time-resolved PL measurements: An excitation source of 375 nm pulsed diode laser (50 ps) was used. A 10× long focus was used to project the incident laser onto the sample and collect the backscattered emission signal. The PL signal was directed into the 300 mm focal length grating spectrograph (HRS-300 MS), where a hybrid photomultiplier detector together with a time-correlated single photon counting electronics (Time Tagger Ultra) was used.

In situ structural characterizations

High-pressure angle-dispersive X-ray diffraction(ADXRD) measurements: The 4W2 High-Pressure Station in the Beijing Synchrotron Radiation Facility performed ADXRD experiments (λ= 0.6199 Å). CeO_2 was used for calibration. The Bragg diffraction rings were collected by a Mar-345 CCD detector and then combined into a

one-dimensional profile using the FIT2D application. The Material Studio application refined the structure.

In situ high-pressure Raman measurements: A Raman spectrometer (iHR 550, Symphony II, Horiba Jobin Yvon) with a 785 nm and 10 mW excitation laser was used to record Raman spectra.

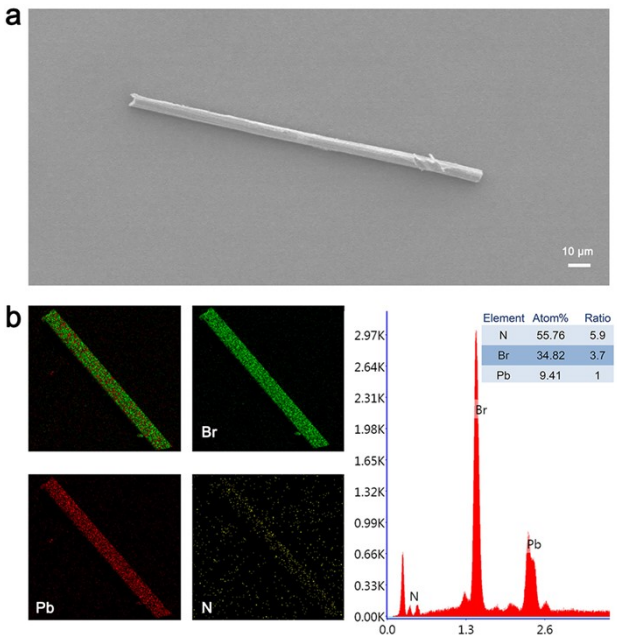

Fig. S1. (a) SEM images of $(HMTA)_3Pb_2Br_7$. (b) Element mapping images and EDS for $(HMTA)_3Pb_2Br_7$.

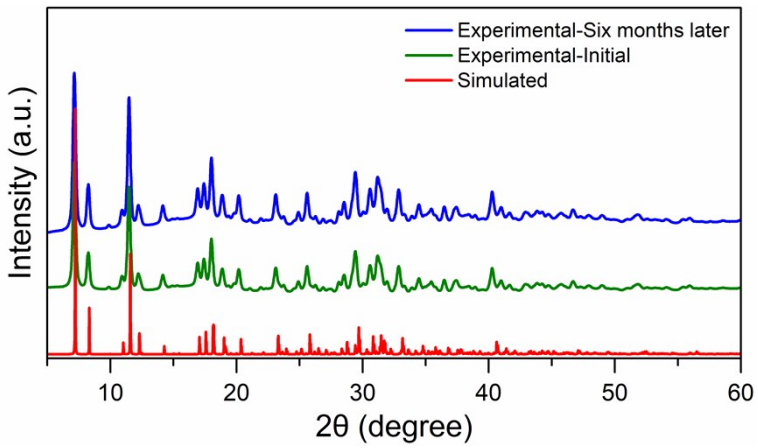

Fig. S2. The powder XRD patterns of $(C_6H_{13}N_4)_3Pb_2Br_7$.

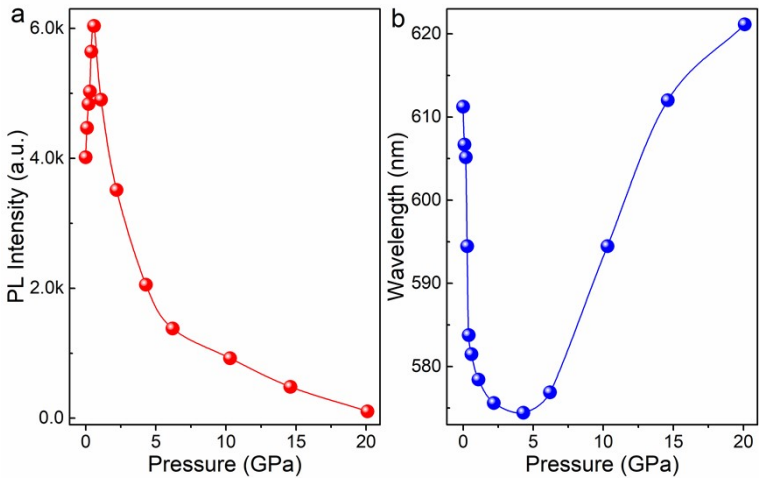

Fig. S3. (a) Pressure-dependent PL intensity evolution of $(HMTA)_3Pb_2Br_7$ crystal. (b) Emission peak location of $(HMTA)_3Pb_2Br_7$ as a function of pressure.

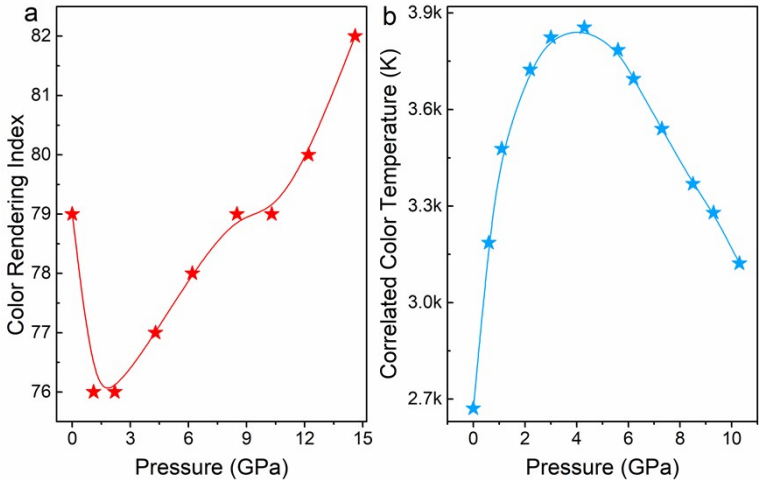

Fig. S4. (a) Pressure-dependent Color rendering index (CRI) of the $(HMTA)_3Pb_2Br_7$ crystal. (b) The change correlated color temperatures (CCT) of $(HMTA)_3Pb_2Br_7$ upon compression.

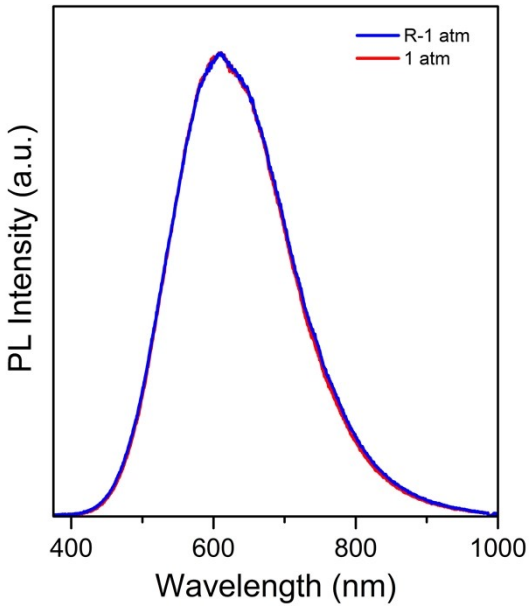

Fig. S5. PL spectra for $(HMTA)_3Pb_2Br_7$ at 1 atm and after releasing pressure at ambient conditions.

Table S1. The regulation of luminous properties of different materials by pressures.

Sample	Pressure range of PL enhancement (GPa)	Structural phase	Phase transition (GPa)	Amorphization (GPa)	References
Mn-doped $CsPbBr_3$ NCs	2.05-14.45	*Pnma*→*Pnma*	2.00	25.6	2
$(BA)_4AgBiBr_8$	1 atm-8.2	*C*2/*m*→*P*2$_1$/*c*	2.1	10.0	3
BA_2PbBr_4	1 atm-0.9	*Pbca*→*P*2$_1$/*c*	0.3	/	4
$PA_8Pb_5I_{18}$	0.0-3.5	*P*2/*c*→*P*2/*c*	3.2	16.0	5
$(PEA)_2PbCl_4$ NCs	1 atm-0.4	*P*-1→*P*-1	2.1	10.0	6
$C_4N_2H_{14}SnBr_4$	0.17-8.01	*I*2/*M*→*P*-1	3.50	14.80	7
$C_4N_2H_{14}PbBr_4$	1.5-2.8	*Imma*→*P*2$_1$/*n*	2.8	/	8
$C_4N_2H_{14}PbBr_4$ NCs	1.75-6.18	*Pnma*→*P*-1	2.66	20.01	9
$CsCu_2I_3$	1 atm-8.0	*Cmcm*→*Pbnm*	8.0	/	10
Cs_4PbBr_6 NCs	0.14-3.01	*R*3*c*→*B*2/*b*	4.01	14.27	11
$(4AMP)_2ZnBr_4$	1 atm-5.07	*P*2$_1$2$_1$2$_1$→*P*2$_1$	5.07	18.17	12
$Cs_2InBr_5{\cdot}H_2O$	6.0-11.0	*Pnma*→*Pnma*	8.3	/	13
$C_5N_2H_{16}Pb_2Br_6$	0.0-2.9	*P*2/*c*	No Phase	/	14
$(C_6H_{13}N_4)_3Pb_2Br_7$	1 atm-0.6	*P*6$_3$/*m*	No Phase	/	This work

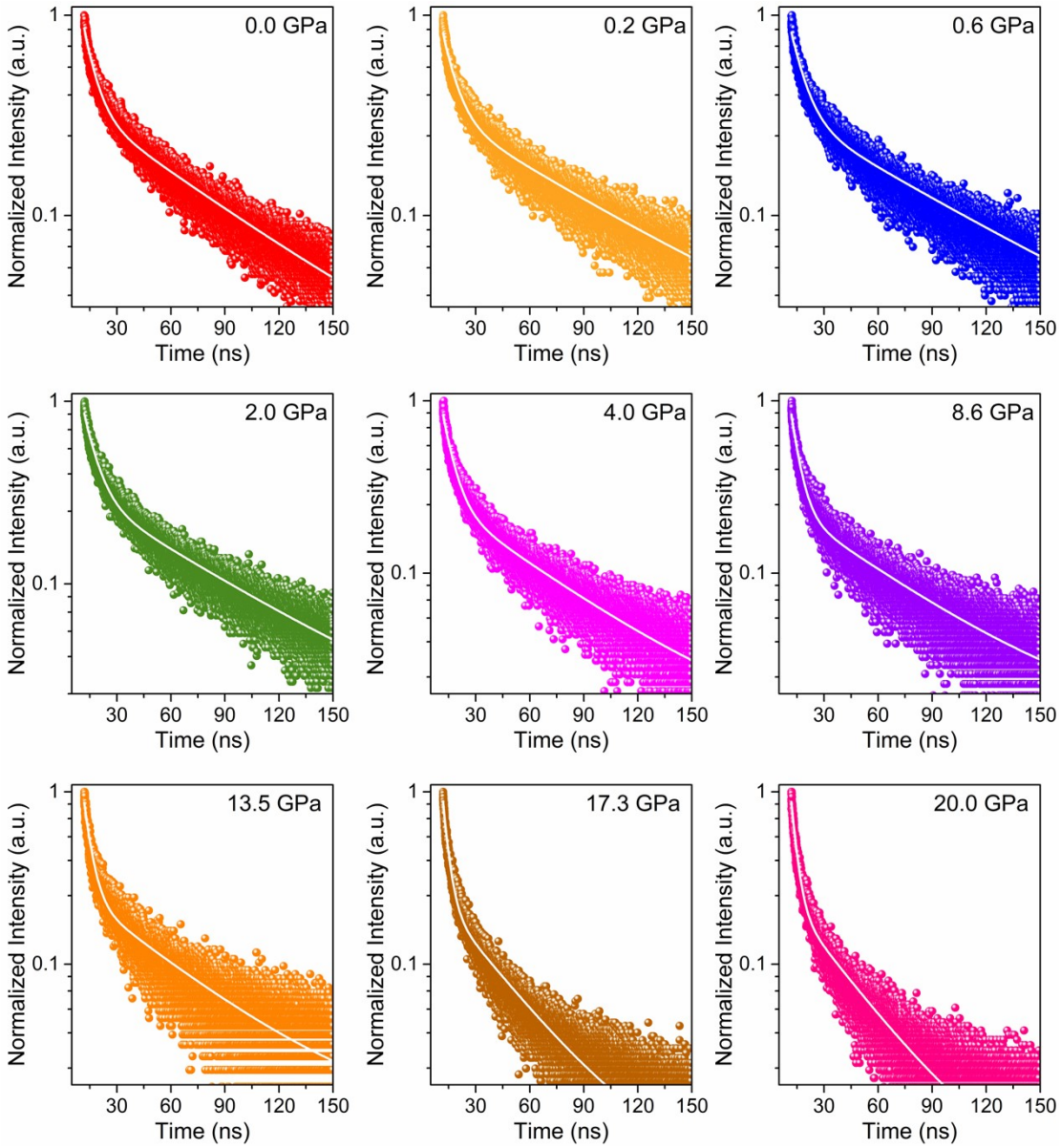

Fig. S6. Time-resolved PL spectra of $(HMTA)_3Pb_2Br_7$ at different pressures.

Table S2. The fast-decay component τ_1, the slow-decay component τ_2, and the average lifetime of $(HMTA)_3Pb_2Br_7$ under different pressure.

Pressure (GPa)	τ_1 (ns)	τ_2 (ns)	Average lifetime (ns)
0.0	6.30	66.99	80.23
0.2	7.00	77.03	92.44
0.4	7.41	79.80	96.94
0.6	7.42	80.78	98.16
1.4	7.36	73.08	91.64
2.0	6.96	69.25	86.35
2.6	6.00	61.09	74.44
3.3	5.57	57.90	69.20
5.1	5.16	56.77	65.95
8.6	4.63	56.42	62.27
10.6	4.37	55.99	60.30
13.5	4.15	51.74	54.61
15.4	3.26	36.64	31.10
17.3	3.12	33.08	26.70
20.0	3.07	31.60	24.77

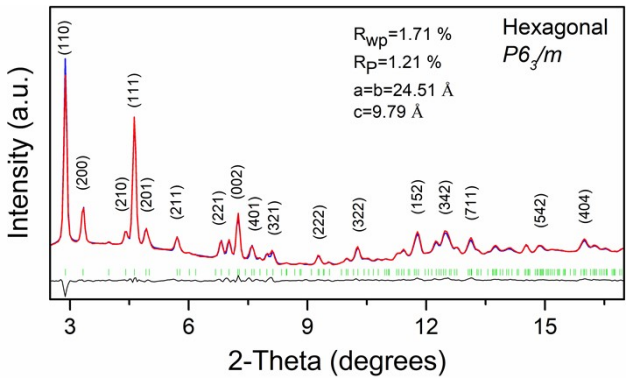

Fig. S7. Rietveld refinement of ADXRD pattern at ambient conditions. Green bars represent the refined peak positions and the black line shows the difference between experimented (blue) and simulated (red) diffraction profiles.

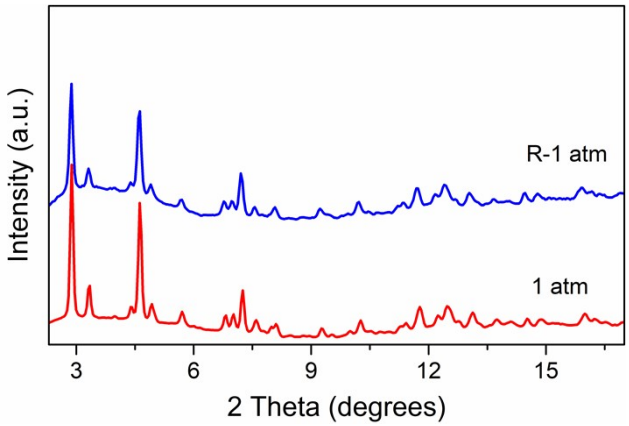

Fig. S8. ADXRD patterns of $(HMTA)_3Pb_2Br_7$ at 1 atm and after releasing pressure.

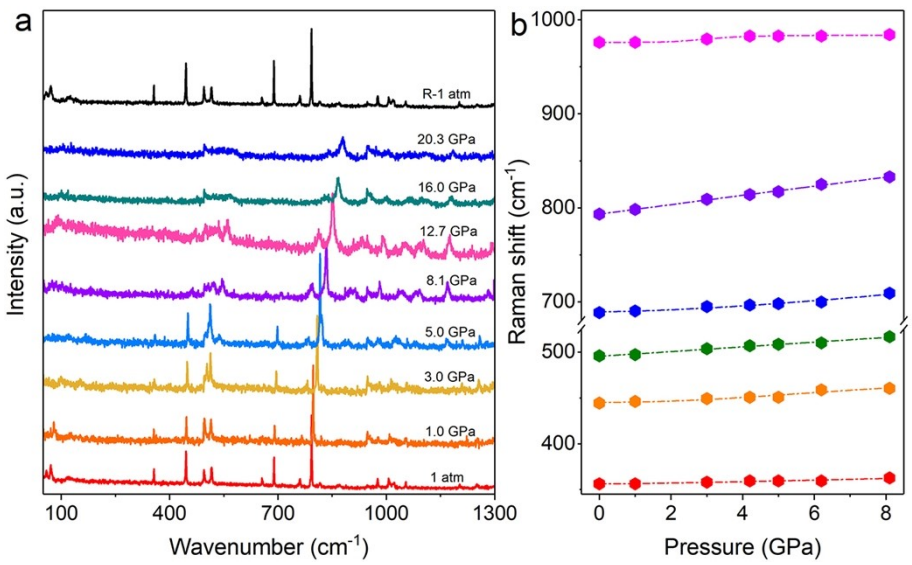

Fig. S9. (a) *In situ* Raman spectra of $(HMTA)_3Pb_2Br_7$ under high pressure, (b) Raman shift of $(HMTA)_3Pb_2Br_7$ as a function of pressure.

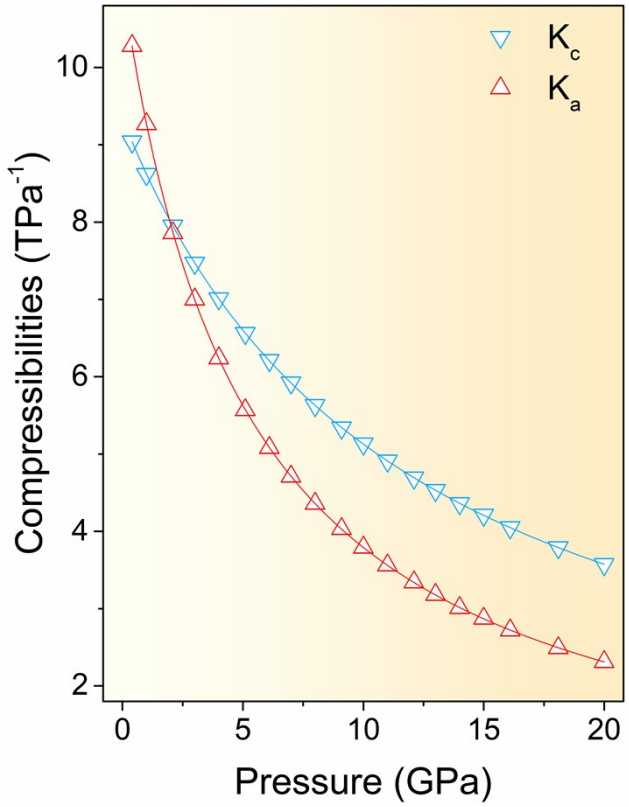

Fig. S10. High-pressure compressibility of the *a* and *c* axes in $(HMTA)_3Pb_2Br_7$.

Table S3. The bulk modulus of perovskite materials with different dimensions.

Dimension	Material	Bulk modulus (GPa)	References
3 D	$MAPbI_3$	4.5	15
	$MASnCl_3$	8.4	16
	$FASnI_3$	8.0	17
	$MA_{0.5}FA_{0.5}SnI_3$	11.5	17
	$FAPbI_3$	11.0	18
	$CsPbI_3$	14.3	19
2 D	$(ETA)_2PbI_4$	22.2	20
	$(BA)_4AgBiBr_8$	10.80	3
	$(PEA)_2PbBr_4$	20.29	21
	$(HA)_2(GA)Pb_2I_7$	15.5875	22
	$Cs_2PbI_2Cl_2$	16.8	23
	$PA_8Pb_5I_{18}$	46.4	5
1 D	$C_4N_2H_{14}SnBr_4$	13.20	7
	$C_5N_2H_{16}Pb_2Br_6$	14.7	14
	$C_4N_2H_{14}PbBr_4$	18.8	8
	$C_4N_2H_{14}PbCl_4$	20.4	24
	$CsCu_2I_3$	25.18	10
	$(C_6H_{13}N_4)_3Pb_2Br_7$	35.16	This work

Table S4. The Br-Pb-Br angles for $(HMTA)_3Pb_2Br_7$ under different pressure.

Bond angle	0.0 (GPa)	1.0 (GPa)	2.0 (GPa)	4.0 (GPa)	6.0 (GPa)	8.0 (GPa)	10.0 (GPa)
Br1-Pb1-Br3 (degree)	92.31	91.05	90.86	89.79	88.18	87.31	87.19
Br3-Pb1-Br4 (degree)	85.02	84.98	84.83	84.31	83.70	82.99	82.90
Br2-Pb2-Br4 (degree)	88.05	86.66	86.43	81.95	78.36	77.98	77.80
Br3-Pb2-Br4 (degree)	85.15	85.07	84.55	83.56	82.78	82.60	82.51

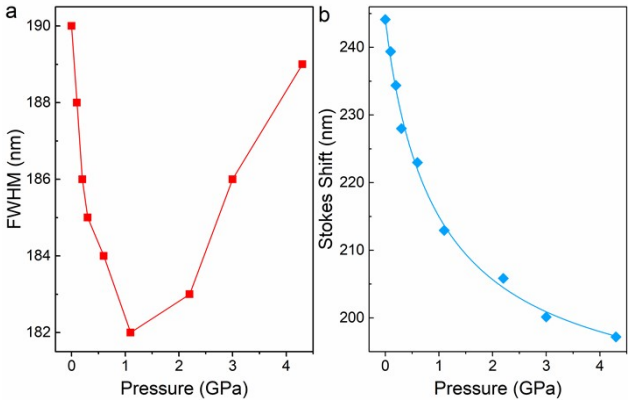

Fig. S11 (a) Pressure-induced Full width at half-maximum (FWHM) change of $(HMTA)_3Pb_2Br_7$. (b) Stokes shift variation with increasing pressure.

References

1. Lin, H.; Zhou, C.; Tian, Y.; Besara, T.; Neu, J.; Siegrist, T.; Zhou, Y.; Bullock, J.; Schanze, K. S.; Ming, W.; Du, M.H.; Ma, B. Bulk assembly of organic metal halide nanotubes. *Chem. Sci.* 2017, **8** (12), 8400-8404.
2. Y. Shi, W. Zhao, Z. Ma, G. Xiao and B. Zou, *Chem Sci*, 2021, **12**, 14711-14717.
3. Y. Fang, L. Zhang, L. Wu, J. Yan, Y. Lin, K. Wang, W. L. Mao and B. Zou, *Angew. Chem. Int. Ed.*, 2019, **58**, 15249-15253.

4. P. Shen, T. Vogt and Y. Lee, *J Phys Chem Lett*, 2020, **11**,4131-4137.
5. Y. Liang, M. Wu, C. Tian, X. Huang, Y. Huang, Y. Lekina, Z. X. Shen and X. Yang, *ACS Applied Energy Materials*, 2021, 1c01925.
6. R. Fu, W. Zhao, L. Wang, Z. Ma, G. Xiao and B. Zou, *Angew. Chem. Int. Ed.,* 2021, 15395.
7. Y. Shi, Z. Ma, D. Zhao, Y. Chen, Y. Cao, K. Wang, G. Xiao and B. Zou, *J Am Chem Soc*, 2019, **141**, 6504-6508.
8. Y. Wang, S. Guo, H. Luo, C. Zhou, H. Lin, X. Ma, Q. Hu, M. H. Du, B. Ma, W. Yang and X. Lu, *J Am Chem Soc*, 2020, **142**, 16001-16006.
9. Z. Ma, F. Li, L. Sui, Y. Shi, R. Fu, K. Yuan, G. Xiao and B. Zou, *Advanced Optical Materials*, 2020, 00713.
10. Q. Li, Z. Chen, B. Yang, L. Tan, B. Xu, J. Han, Y. Zhao, J. Tang and Z. Quan, *J Am Chem Soc*, 2020, **142**, 1786-1791.
11. Z. Ma, Z. Liu, S. Lu, L. Wang, X. Feng, D. Yang, K. Wang, G. Xiao, L. Zhang, S. A. T. Redfern and B. Zou, *Nat Commun*, 2018, **9**, 4506.
12. D. Zhao, G. Xiao, Z. Liu, L. Sui, K. Yuan, Z. Ma and B. Zou, *Adv Mater*, 2021, e2100323.
13. Q. Li, B. Xu, Z. Chen, J. Han, L. Tan, Z. Luo, P. Shen and Z. Quan, *Advanced Functional Materials*, 2021, **8**, 2104923.
14. H. Luo, S. Guo, Y. Zhang, K. Bu, H. Lin, Y. Wang, Y. Yin, D. Zhang, S. Jin, W. Zhang, W. Yang, B. Ma and X. Lu, *Advanced Science*, 2021, 202100786.
15. F. Capitani, C. Marini, S. Caramazza, P. Postorino, G. Garbarino, M. Hanfland, A. Pisanu, P. Quadrelli and L. Malavasi, *Journal*, 2016, 316-16411.
16. L. Wang, T. Ou, W. Kai, G. Xiao, C. Gao and Z. Bo, *Applied Physics Letters*, 2017, **111**, 233901.
17. Y. Lee, D. B. Mitzi, P. W. Barnes and T. Vogt, *Physical Review B*, 2003, **68**, 366-369.
18. G. Liu, L. Kong, J. Gong, W. Yang, H. K. Mao, Q. Hu, Z. Liu, R. D. Schaller, D. Zhang and T. Xu, *Advanced Functional Materials*, 2017, **27**, 1604208.
19. G. Yuan, S. Qin, X. Wu, H. Ding and A. Lu, *Phase Transitions*, 2017, 1-10.

20. Y. Fang, L. Zhang, Y. Yu, X. Yang, K. Wang and B. Zou, *CCS Chemistry*, 2021, **2**, 2203-2210.
21. L. Zhang, L. Wu, K. Wang and B. Zou, *Advanced Science*, 2019, **6**, 1801628.
22. S. Guo, Y. Zhao, K. Bu, Y. Fu, H. Luo, M. Chen, M. P. Hautzinger, Y. Wang, S. Jin, W. Yang, X. Lü, *Angew. Chem. Int. Ed.*, 2020, 59, 17533.
23. S. Guo, K. Bu, J. Li, Q. Hu, H. Luo, Y. He, Y. Wu, D. Zhang, Y. Zhao, W. Yang, M. G. Kanatzidis and X. Lu, *J Am Chem Soc*, 2021, **143**, 2545-2551.
24. Y. Fang, T. Shao, L. Zhang, L. Sui, G. Wu, K. Yuan, K. Wang and B. Zou, *JACS Au*, 2021, **1**, 459-466.